






RESEARCH ARTICLE

# Study of the applicability of radio signals emitted by lightning for long-range navigation

Pavel Kovář,  Pavel Puričer,  and Jan Mikeš 

Faculty of Electrical Engineering, Czech Technical University in Prague, Prague, Czech Republic.

**Corresponding author:** Pavel Kovář; Email: [kovar@fel.cvut.cz](mailto:kovar@fel.cvut.cz)

**Received:** 15 June 2021; **Accepted:** 3 January 2024

**Keywords:** lightning discharge; lightning radio pulse; signals in opportunity; VLF navigation

## Abstract

The complementary radio navigation system based on the Very Low Frequency signals produced by lightning is an alternative to today's Global Navigation Satellite Systems. The system operates on different principles and uses different radio frequency bands. The signals have higher availability in problematic places. The analyses based on the historical data of World Wide Lightning Location Network demonstrated the good availability of the service, sufficient number of lightning strokes and good geometry calculated for a 10-second time window for positioning based on the Time of Arrival principle. The geometry was evaluated with the help of the Geometric Dilution of Precision coefficient. The Geometric Dilution of Precision median for the reception of the lightning signal from a range of 10,000 km moves around one except at the southern polar regions and the probability of the service availability exceeds 80%.

## 1. Introduction

Since ancient times, humankind has been afraid of lightning because it ignites their homes, causes fires and, more recently, the strokes damage electrical and electronic devices, aircrafts, ships and other transportation modes (Rakov and Uman, 2007; Parmantier et al., 2012). Lightning is being scientifically researched and protection methods are being developed but people still have so far failed to tame lightning or put it to practical use (Bazelyan and Raizer, 2000; Horvat, 2006; Cooray, 2010).

A lightning stroke generates Very Low Frequency (VLF) pulses of high energy that propagate through tens of thousands of kilometres and can be used for radio navigation based on the Time of Arrival (ToA) principle.

### 1.1. Phenomenology of lightning occurrence

A key parameter to assess the number of events related to a lightning discharge is a thunderstorm day  $T_d$  often called the keraunic level. The thunderstorm day is defined as a local calendar day during which at least one lightning stroke has been observed at a given location. This value is regularly increased thanks to technical improvements of the methods of the position determination of individual lightning flashes. With the technical development of monitoring stations, their density and the time of statistical processing, this number becomes an important parameter. The number of thunderstorm days  $T_d$  can be further recalculated from the ground flash density  $N_g$  in  $\text{km}^2$  per year. Between ground flash density and thunderstorm days, there can be stated a relationship  $N_g = 0.04 \cdot T_d^{1.25}$ . This formula was adopted by the Institute of Electrical and Electronics Engineers (IEEE) and implemented in many engineering

standards. There exist plenty of lightning detection networks that provide information about  $T_d$  and  $N_g$ . Our research works with the use of the World Wide Lightning Location Network (WWLLN).

### 1.2. Lightning parameters from an engineering point of view

The most studied part of a lightning process is the return stroke (return streamer). Its current is the most readily identifiable source of an electromagnetic pulse and the most common cause that contributes to damage of lightning-affected objects. From the mathematical and technical points of view, the return stroke can be described as an exponential curve – the so-called Heidler function in Equation (1). This formula was accepted by the International Electrotechnical Commission (IEC) for all the standards. The special type of return streamer of cloud-to-ground discharges is very intense because of the high electrical conductivity of the ground, and hence this type of streamer is not to be found in air discharges, cloud discharges or cloud-to-cloud discharges.

The return stroke produces almost all of the luminosity and charge transfer in most cloud-to-ground strokes. A typical current amplitude is  $3 \times 10^4$  A and the ascent speed is typically  $10^8$  m/s. The discharge process of the return stroke is completed in a few tens of microseconds. The IEC standards for lightning protection define typical values of Heidler function constants for modelling dangerous strokes in different protection levels. The peak current varies from 30 to 200 kA. The typical value of  $T_1$  is  $10 \mu\text{s}$  and  $T_2$  is  $350 \mu\text{s}$ .

The return stroke can then be expressed as

$$i = \frac{I}{k} \cdot \frac{\left(\frac{t}{T_1}\right)^{10}}{1 + \left(\frac{t}{T_1}\right)^{10}} \cdot \exp\left(-\frac{t}{T_2}\right) \quad (1)$$

where  $k$  is the correction factor for the peak current, typically  $k = 0.93$ .

### 1.3. Lightning radio emission

Lightning generates broadband electromagnetic pulses in various frequencies from DC to several Gigahertz (Sonnadara et al., 2006). For the purposes of this paper, we will take into account the VLF pulse only, as the radio pulses of higher frequencies have their reasonable propagation limited to short distances or on the line of sight only.

The strongest component of the spectrum is located around 10 kHz (VLF frequency band). These VLF signals are generated by a return stroke current pulse (Figure 1) that flows through the ionised channel with a length of hundreds of metres or several kilometres (Rakov and Uman, 2007; Lewin et al., 2008). This channel then works from the radio transmission point of view as a line antenna. The emitted VLF wave propagates on distances of up to several ten thousand kilometres (Chapman et al., 1966; Shao and Jacobson, 2009; Hou et al., 2018). The typical energy of the lightning is 10 GJ (Bermudez et al., 2004). If only a small part of this energy converts to the radio impulse, the energy of this broadcast impulse is in the rank of tens of MJ.

The radio signals produced by lightning are used for the localisation of the lightning discharges or for the study of the physical processes in the thunderstorm clouds. For this purpose, several professional or semi-professional lightning detection networks have been built (Hutchins et al., 2012; Klimov et al., 2018; Narita et al., 2018). The lightning detection networks mainly operate on the Time Difference of Arrival (TDoA) principle.

For the study of the preliminary processes in the thunderstorm clouds, interferometric directional finders that operate in very high (VHF) or ultra-high (UHF) frequency bands have been developed (Sun et al., 2013; Rison et al., 2016; Liu et al., 2018).

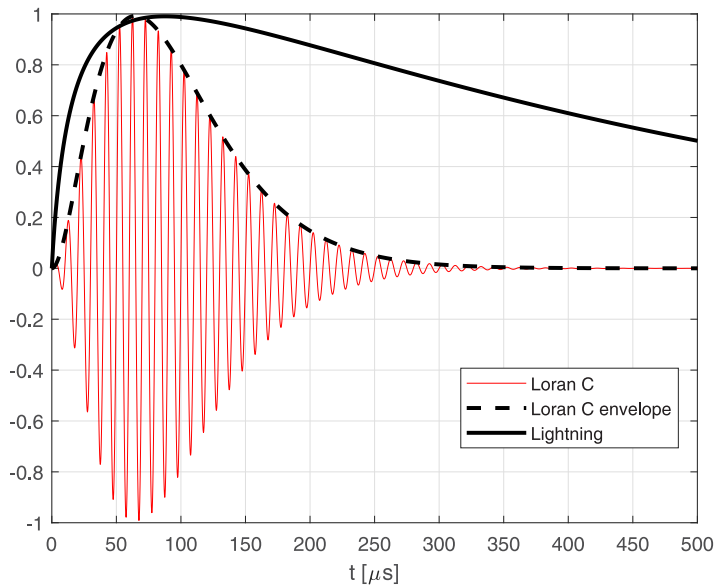


**Figure 1.** Comparison of the normalised lightning current wave and Loran C signal.

#### 1.4. VLF radio navigation systems

For more than a hundred years, humans have been using artificially generated radio signals, which are similar to those produced by lightning, for radio position determination and navigation. One of these systems is Loran C that operates on the 100 kHz carrier frequency and transmits short radio pulses optimised for respectively Time of Arrival and Time Difference of Arrival measurements (Olsen, 1991; Johnson et al., 2005, 2006; Lo et al., 2007). The comparison of the normalised Loran C pulse, its envelope and the return stroke current wave is in Figure 1.

Classical Loran C receivers measure the time of arrival of the signal on the pulse envelope, where the modernised receivers combine envelope and carrier phase measurement. The typical accuracy of the Loran C system varies from 200 to 500 m and it can be improved to tens of metres by a differential measurement (Yuan et al., 2020).

The radiated power of the Loran C transmitters varies from 200 kW to 2 MW. The radiated energy of one Loran C pulse therefore varies from 20 to 200 J.

Since the rising edge of the lightning wave is several times steeper than the Loran C envelope edge, it can guarantee lower noise of the time of arrival estimation than a classical envelope-based Loran C measurement.

The mentioned VLF band (namely frequencies from 10 to 14 kHz) was used by the Omega navigation system (Swanson, 1983; Wenzel, 1989; Warren et al., 1992; Morris and Casswell, 1994; Sakran and Swanson, 1998). The system was global and used only eight transmitters. The range covered by the signals of the transmitters was up to 10,000 km.

The Omega navigation system operated on a slightly different principle when the receiver measures the carrier phase. The receiver measured a carrier phase of the VLF signal. The precision of the original system was 4 nautical miles (7.4 km) and was further gradually improved by the introduction of the signal propagation model (Morris and Casswell, 1994) and by differential measurement methods.

The Omega signals were transmitted by the umbrella antennae with a height of 0.02 of the wavelength ( $\lambda$ ), which leads to the low radiation efficiency of approximately 25–38% (Egashira and Taguchi, 1985). The radiated power was approximately 10 kW.

### 1.5. Complementary radio navigation system

In radio navigation, the Global Navigation Satellite Systems (GNSSs) play the dominant roles thanks to their precision and the small size of the navigation receivers and antennae. The traditional VLF or LF systems have already been decommissioned or are in the process of being put out of operation (Olsen, 1991; Sakran and Swanson, 1998). However, human society has gradually become dependent on technologies, including navigation systems, which raises the issue of backup systems (Johnson et al., 2005) because GNSS systems are relatively easy to jam, their function is affected by space weather, they are problematically available indoors and are often subjects of unwanted interferences with other systems in adjacent frequency bands.

Backup or complementary systems should, if possible, work on other technology, use different principles, and completely different frequency bands and different transmitters in dissimilar locations.

The potential precision of the proposed lightning navigation system would be most likely better than the precision of the vintage VLF navigation systems Omega and Loran C for the following reasons.

- The precision of the measurement of the signal time of arrival is proportional to the energy of the processed signal and inversely proportional to the noise. The energy of the lightning signal that could be used for navigation is a hundred or thousand times higher than the energy of the Loran C pulse.
- The propagation effects in the earth-ionosphere waveguide can be eliminated by local elements that can measure the propagation delay and register the shape of the VLF wave of the individual lightning and provide this information to the users, e.g. in the form of differential corrections or an augmentation message.
- The system can apply the advanced signal processing methods based on a utilisation of the information of the individual lightning waves registered by local elements for an improvement of the precision of the ToA estimation.

The aim of this paper is to investigate the geometry and signal availability of lightning for radio navigation. In Section 2, the GDOP coefficient that measures the quality of positions of the navigation sources is introduced. Section 3 provides an analysis of the GDOP coefficient from the lightning location data measured by the WWLLN in 2019. Finally, Section 4 summarises the research results and introduces some remarks and notes on a possible implementation.

## 2. Materials and methods

The navigation receiver based on the ToA method measures the time of arrival  $t_{r,i}$  of the  $i$ th navigation signal to the receiver clock (Johnson et al., 2006; Chen et al., 2013). The user position and time are then estimated from the geometry of the navigation task and times of arrival using one of the known approaches: least square in Equation (2) or weighted least square methods or by a navigation filter like Kalman or Extended Kalman. The mentioned methods are based on linearisation of the problem in the vicinity of a user in a set of position equations in the matrix form below:

$$\begin{matrix} & \mathbf{H} & & \delta \mathbf{r} & & \delta t_r \\ & \left[ \begin{array}{ccc} \sin \varphi_1 & \cos \varphi_1 & 1 \\ \sin \varphi_2 & \cos \varphi_2 & 1 \\ \vdots & \ddots & \vdots \\ \sin \varphi_n & \cos \varphi_n & 1 \end{array} \right] & \begin{bmatrix} \delta x \\ \delta y \\ c \delta t \end{bmatrix} & = & \begin{bmatrix} \delta t_{r,1} \\ \delta t_{r,2} \\ \vdots \\ \delta t_{r,n} \end{bmatrix} \\ & & & & & (2) \end{matrix}$$

where  $\mathbf{H}$  is the directional cosines matrix,  $\varphi_i$  is the angle of arrival of the  $i$ th signal,  $c$  is the speed of light and  $\delta x$ ,  $\delta y$ ,  $\delta t$  are differentials of the user position and time.

The directional cosine matrix is calculated from the known positions of the signal sources. In the case of using the signal of opportunity like lightning strokes, the system must be augmented by the entities that measure the time and position of the generation of the navigation signals.

The precision of the position determination depends on the precision of the  $t_{r,i}$  time of arrival measurement, propagation effects, and on the matrix  $\mathbf{H}$  that takes into account the number of the navigation signals and positions of the signal sources.

The quality of positions of the signal sources (geometry) is measured by DOP coefficients like GDOP (Geometric Dilution of Precision) in Equation (4) that are calculated from the covariance matrix in Equation (3). The unity standard deviation ( $\sigma = 1$ ) of the measurement is assumed.

$$\mathbf{C}_{\delta r} = (\mathbf{H}^T \mathbf{H})^{-1} \cdot \sigma^2 \quad (3)$$

$$\text{GDOP} = \sqrt{\text{tr}[(\mathbf{H}^T \mathbf{H})^{-1}]} \quad (4)$$

### 2.1. Navigation service availability

Under the term availability of navigation services, we will understand the navigation signals' availability and their good geometry. In traditional radio navigation systems, the transmitters' signal availability and geometry are ensured by the system provider. The only unknown parameters are propagation conditions and jamming. In addition, the provider can choose the right frequency band with stable radio wave propagation and low noise and interference.

In the case of lightning radio pulses, which are natural signals, people can influence neither the time of lightning nor its position. The signal availability can be statistically estimated from the long-term lightning location data provided by global lightning networks like WWLLN (Hutchins et al., 2012), Vaisala Global Lightning Detection Network GLD360 (Lojou et al., 2011) or Blitzortung (Narita et al., 2018). Some global lightning data are also collected by satellites (Christian et al., 2003; Klimov et al., 2018).

The big advantage of the navigation systems based on VLF lightning pulses is the fact that an illegal attack on the lightning is practically impossible. In contrast, the jamming or denial of the navigation radio beacons and infrastructure is well imagined.

For estimation of the navigation service availability and quality of the geometry of the navigation task, the software scripts for the Matlab environment have been developed and were used to produce further presented results. The software calculates a number of visible signals and GDOP parameters from the historical WWLLN data. The availability statistics are calculated for the  $\varphi_{grid}$ -degree geographic grid. The GDOP is investigated in the  $T_w$  time window. Data are then statistically analysed and interpreted in Section 3. The reception range (visibility) of the signal is defined by the so called visibility angle  $\Theta_{vis}$ . The processing software calculates the angle between the user position vector and lightning position vector in the Earth-Centred Earth-Fixed (ECEF) coordinate system. The lightning is visible for an angle lower than  $\Theta_{vis}$  and vice versa.

The visibility angle for a definition of the propagation range was selected instead of the range itself to simplify the calculations. For the decision, of whether the lightning is visible or not, we just calculate the position vector of the user and the position vector of the lightning in ECEF coordinates, and then the visibility angle is calculated from the vector products of these two vectors. As the Equator circumference is approximately 40,000 km, the visibility angles  $90^\circ$  and  $45^\circ$  correspond to 10,000 and 5,000 km, respectively.

## 3. Results and discussion

This section presents an estimation of the signal geometry and service availability based on the lightning location data measured by the WWLLN in 2019. The WWLLN data provider declares that the network detects approximately 30% of lightning of current greater than 30 kA. In addition, the network stations

**Table 1.** Number of detected lightning events in a ten-second window.

Month	Min.	Max.	Mean	Median
January	26	117	65	65
February	20	141	67	67
March	33	147	81	81
April	36	145	80	79
May	31	132	74	74
June	37	136	78	77
July	33	129	72	71
August	28	120	67	66
September	26	133	71	70
October	27	130	70	70
November	33	131	75	74
December	26	133	69	69
Year 2019	20	150	71	71

are not distributed uniformly; therefore, the detection efficiency can vary with the geographic position. With respect to these current limitations, the reality could be likely a little bit better than presented in this paper.

The DOP is calculated for 10 s windows ( $T_w = 10$  s), data are processed for two visibility angles  $\Theta_{vis}$  45° and 90° which correspond to the ranges 5,000 and 10,000 km, respectively. The value of 10 s for the time window was chosen as a model value to respect the average application for the receiver with ordinary movement patterns typical for road transport (car, truck) in open terrain (outside urban environment with sharp turns and sudden stops). The one extreme can be a fighter jet changing the trajectory in a fraction of a second, the other is a big cargo vessel with slow movement and turns. The calculation of the matrix inversion of a large frequently nearly singular matrix in Equation (3) brings high demands to computational power and a challenge of optimising the processing algorithms, even in the case of the use of the supercomputer centre of the Czech Technical University. To demonstrate the viability of the presented concept, the dataset was reduced to the first and fifteenth day of each month.

Table 1 shows a basic statistic concerning the number of lightning events that occurred globally in the 10-second window splits for individual months of 2019. The number of events (flashes) varied from 20 to 150. The median and variance are nearly equal and vary from 65 to 80 events. The values in Table 1 do not carry information about the positions of the lightning.

For radio navigation, not only is the number of available navigation signals important but also the positions of the signal sources. This impact is described by the GDOP coefficient (see Section 2), which represents the value of how many times the error of position is worsened by the system constellation geometry in comparison to the basic measurement error of the time of arrival of the signal. The lower GDOP value represents the better constellation of the signal sources.

The experimental Cumulative Distribution Functions (CDFs) of the GDOP for ranges 10,000 and 5,000 km for 12 positions at the Globe shown in Figure 2 are in Figures 3 and 4. The individual curves express the probability that the GDOP coefficient is lower or equal to the value on the horizontal axis. As this probability depends on the user position, time (month) and maximum propagation range, we plotted two figures with subpanels.

The evaluated positions are uniformly distributed on the equator and forty-fifth parallels of southern and northern latitudes.

It is evident that for the range of 10,000 km, the probability that the GDOP coefficient is low is relatively high. A little worse results were reached in January at the equator or the southern hemisphere. The reason could be a worse WWLLN coverage in this region. The considerably higher calculated GDOP



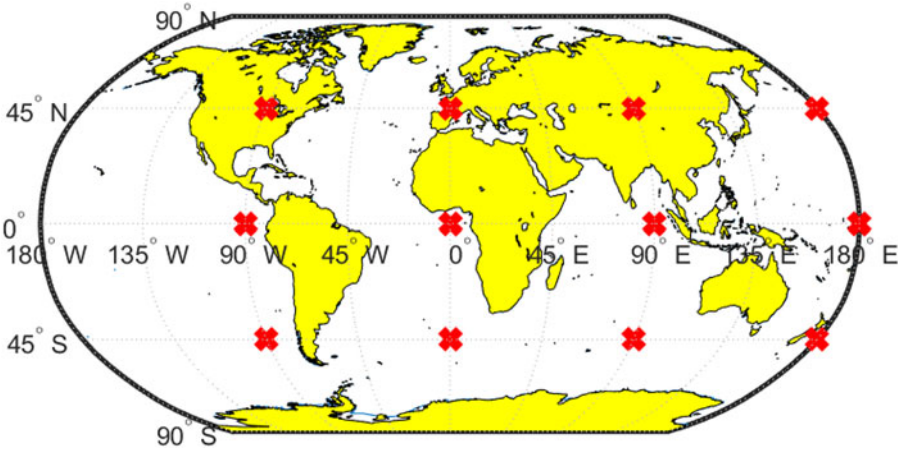


Figure 2. Setup of points for GDOP CDF evaluation.

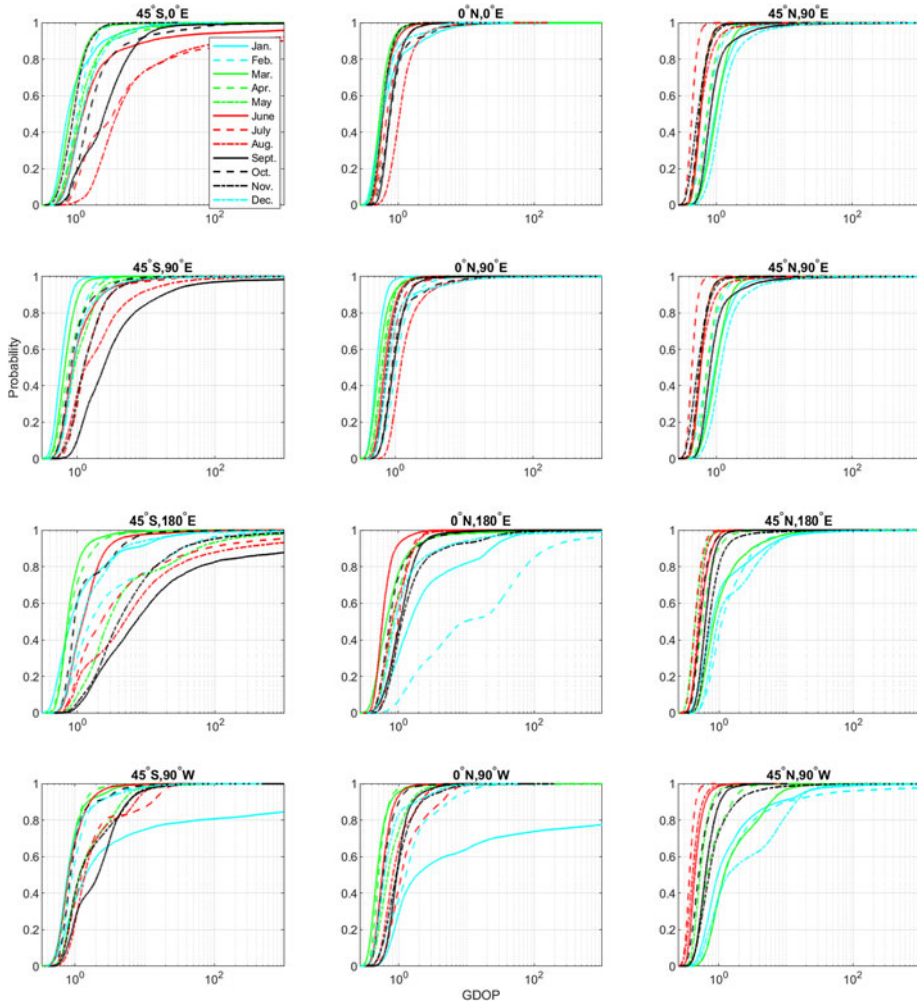
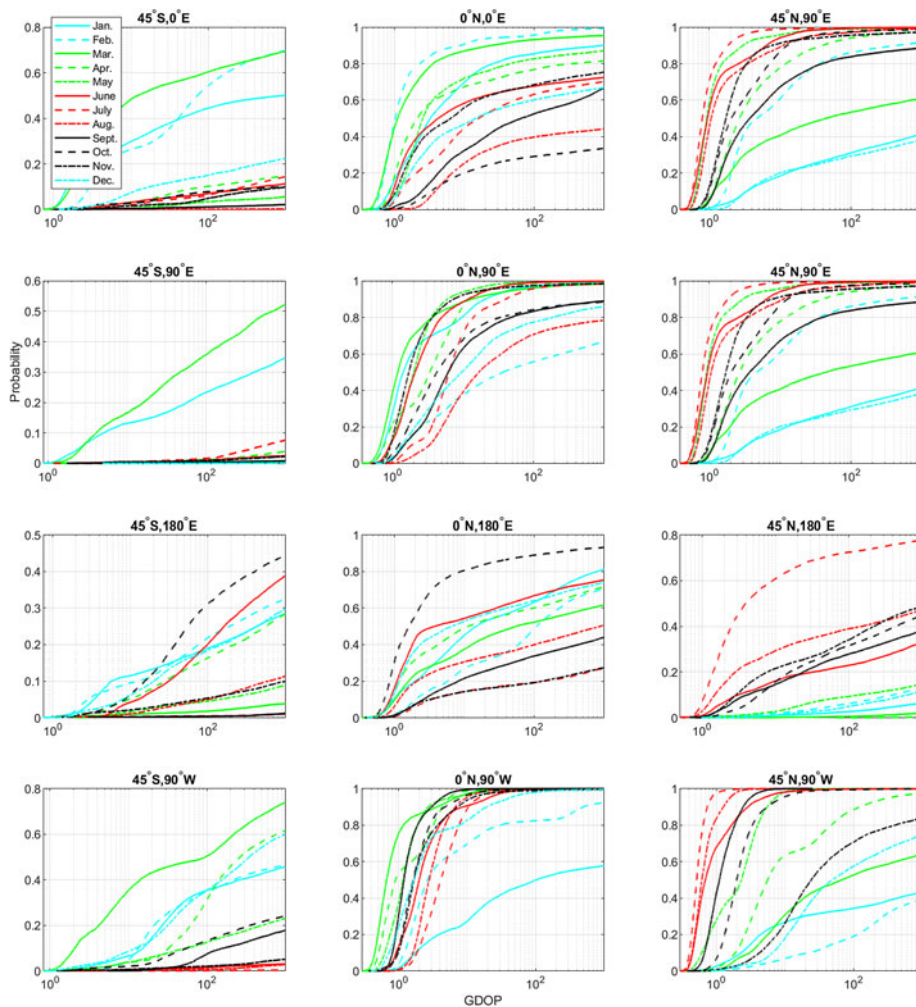


Figure 3. GDOP cumulative distribution function for range 10,000 km.



**Figure 4.** GDOP cumulative distribution function for range 5,000 km.

was observed for the range of 5,000 km. The results show seasonal and geographical dependence. For instance, the GDOP is very high in the middle of the Indian Ocean at coordinates 45°S, 90°E, where the GDOP for the whole year except January and March is very high.

In general, it can be said that in the studied points in the southern hemisphere, GDOP was higher than in the northern hemisphere, regardless of the season. This can be explained both by the lower detection sensitivity of the WWLLN in the southern hemisphere and by the fact that the intensity of lightning strokes is higher above land than above sea (Albrecht et al., 2016), respecting the significantly higher area of the oceans in the southern hemisphere than in the northern.

A similar phenomenon, but less intense, was observed for the season dependence in the northern hemisphere as well. The GDOP was lower in the summer and autumn than in the winter. Large differences between the winter and summer months were observed in the Pacific.

In Figures 5 and 6, there is a median value of the GDOP for the range 10,000 km, respectively 5,000 km, as a function of month and location. Median reaches low values of less than 1 for a range of 10,000 km for most of the year and locations with the exception of the southern polar regions. In these areas, the median GDOP increases, especially in the winter months of June to September, over the value of 5.



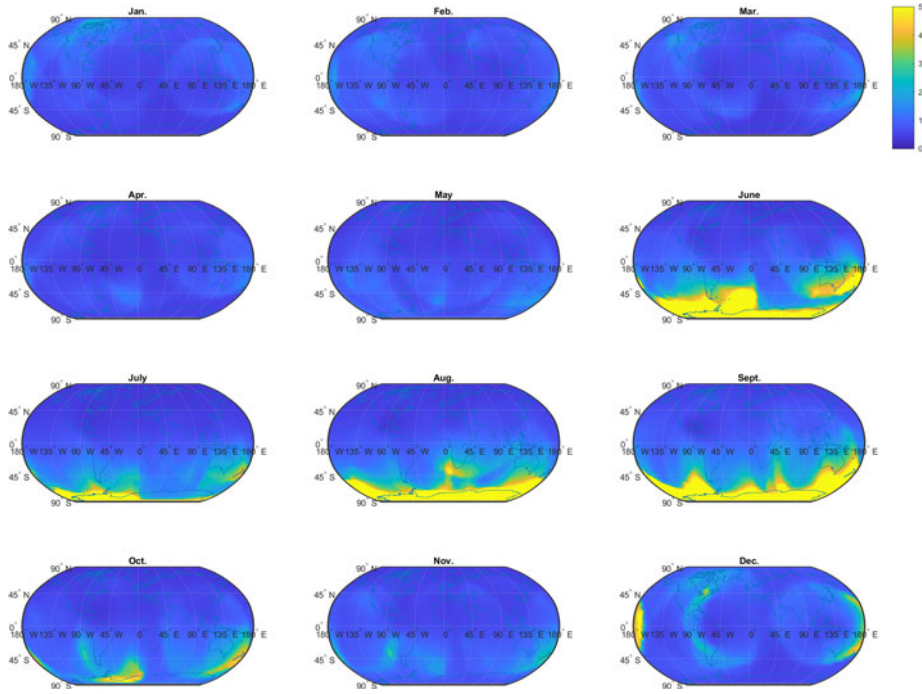


Figure 5. Median of GDOP for range 10,000 km.

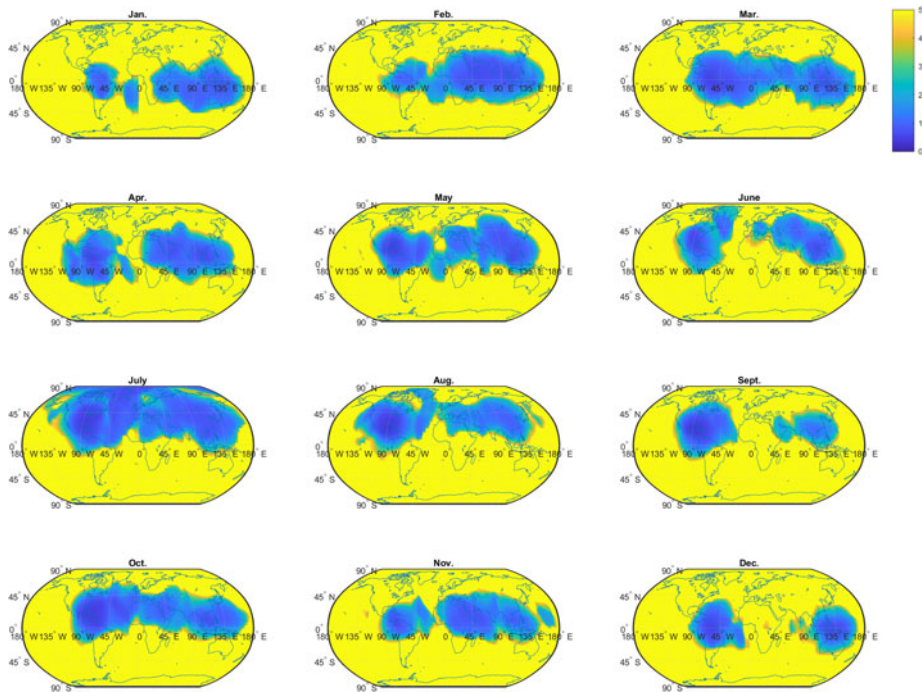
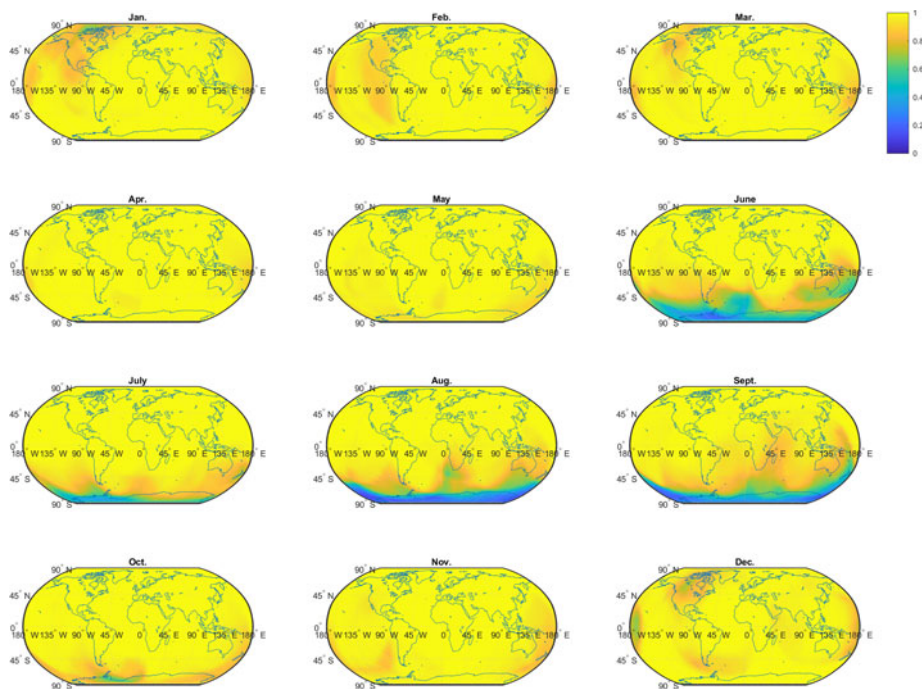


Figure 6. Median of GDOP for range 5,000 km.



**Figure 7.** Probability that GDOP is less than 10 for range 10,000 km.

If we consider a range of only 5,000 km, the median GDOP is significantly higher than in the previous case and exceeds the value of 5 in most of the world. The exceptions are North Africa, South Asia and Central America. Low levels of the median GDOP were also observed over the mainland of the northern hemisphere in July, even at high latitudes.

Figures 7 and 8 show the probability that the GDOP will reach a value less than 10. We set the value of 10 as the limiting value of the system's usability (the position error will not be worse than ten times the error of the measurement). Although we limit the usability of the system by the value of GDOP lower than 10, the median values are depicted in scale up to GDOP of 5 for the sake of picture readability and the full scale impact is shown in Figures 7 and 8.

If we consider a range of 10,000 km, the probability that the value of GDOP will be smaller, and thus the system can be used almost everywhere, is higher than 80%. The exception is a combination of the southern polar regions and the winter months. If we consider a range of up to 5,000 km, it is significantly worse with regards to the service availability. The service is well available in the equatorial areas above the mainland and in July, also over the mainland part of the northern hemisphere.

#### 4. Conclusions

The study proves the applicability of the radio signals produced by lightning for radio navigation. If the signal processing methods are capable of processing signals from 10,000 km distances, the service availability is relatively high, see Figure 5 or 7. The signals are generated by natural phenomena that humans can neither control nor avert.

Illegal attacks and jamming of the system are complicated due to the application of the low-frequency bands and the high energy of the lightning discharges.

During the development and implementation of such a complementary navigation system, several main challenges have to be solved.

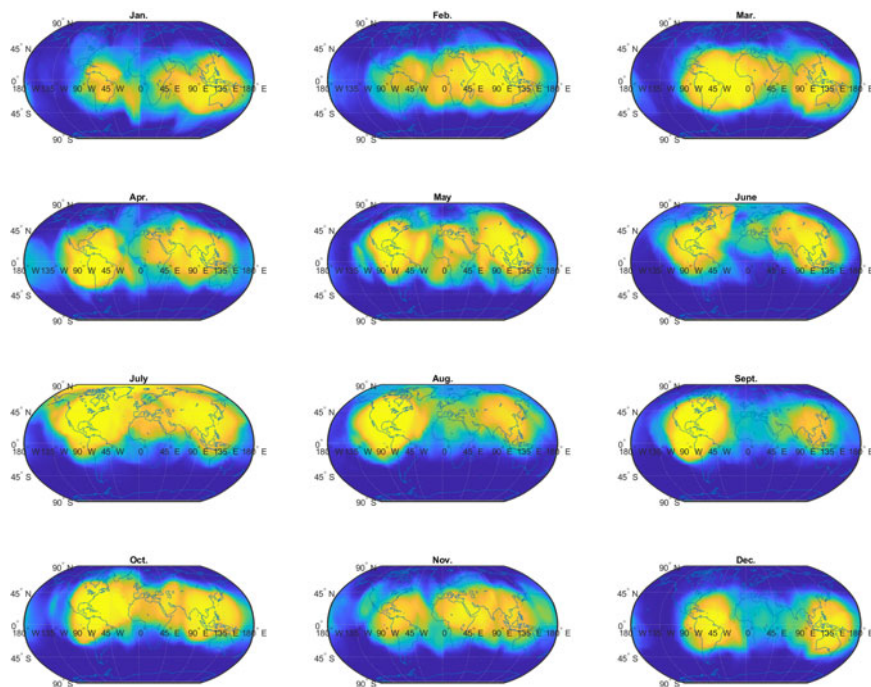


**Figure 8.** Probability that GDOP is less than 10 for range 5,000 km.

It would be necessary to develop and operate a global network for monitoring lightning. The secondary function of the network will be the measurement of the propagation delay of the lightning signals in the waveguide ionospheric channel.

This communication network can be a weak point in the jamming resistance of the whole system. However, there already exist several proven methods to prevent interference or jamming of the communication signal, for example, a spread spectrum technology.

The development of the systems also leads to the development and implementation of highly precise algorithms to measure the time of arrival of the signal to the receiver. These algorithms likely should consider the waveform of the individual lightning registered by the network to improve the precision of estimation of the time of arrival of the signal.

The proposed complementary navigation system is based on the radio signals produced by lightning, and operates on a different principle and frequency band than the presently used GNSS systems. The signal is well-available indoors and even under the water. The first idea about the precision, based on comparison with the existing VLF systems, is within hundreds of metres, which is much higher than the GNSS alternatives.

The utilisation of natural signals for navigation could be an interesting alternative to the global terrestrial network of navigation radio beacons.

**Acknowledgements.** The research was supported by the European Regional Development Fund-Project CRRAT No. CZ.02.1.01/0.0/0.0/15003/0000481.

## References

- Albrecht R. I., Goodman S. J., Buechler D. E., Blakeslee R. J. and Christian H. J. (2016). Where are the lightning hotspots on earth? *Bulletin of the American Meteorological Society*, **97**(11), 2051–2068.
- Bazelyan E. M. and Raizer Y. P. (2000). *Lightning Physics and Lightning Protection* (1st ed.). Boca Raton, FL: CRC Press.
- Bermudez J. L., Rachidi F., Rubinstein M., Janischewskyj W., Shostak V. O., Pavanello D., Chang J. S., Hussein A. M., Nucci C. A. and Paolone M. (2004). Far-field-current relationship based on the TL model for lightning return strokes to elevated strike objects. *IEEE Transactions on Electromagnetic Compatibility*, **47**(1), 146–159.

- Chapman F. W., Jones D. L., Todd J. D. W. and Challinor R. A. (1966). Observations on the propagation constant of the earth-ionosphere waveguide in the frequency band 8 c/s to 16 kc/s. *Radio Science*, **1**(11), 1273–1282.
- Chen Ch. S., Chiu Y. J., Lee Ch. T. and Lin J. M. (2013). Calculation of weighted geometric dilution of precision. *Journal of Applied Mathematics*, **2013**, 953048.
- Christian H. J., Blakeslee R. J., Boccippio D. J., Boeck W. L., Buechler D. E., Driscoll K. T., Goodman S. J., Hall J. M., Koshak W. J., Mach D. M. and Stewart M. F. (2003). Global frequency and distribution of lightning as observed from space by the Optical Transient Detector. *Journal of Geophysical Research*, **108**(D1), 4-1–4-15.
- Cooray H. (2010). *Lightning Protection*. London, UK: The Institution of Engineering and Technology.
- Egashira S. and Taguchi M. (1985). Analysis of umbrella antenna at the omega navigation station. *IEEE Transactions on Antennas and Propagation*, **33**(12), 1401–1403.
- Horvat T. (2006). *Understanding Lightning and Lightning Protection*. Hoboken, NJ: John Wiley & Sons.
- Hou W., Zhang Q., Zhang J., Wang L. and Shen Y. (2018). A new approximate method for lightning-radiated ELF/VLF ground wave propagation over intermediate ranges. *International Journal of Antennas and Propagation*, **2018**, 9353294.
- Hutchins L. M., Holzworth L. H., Brundell J. B. and Rodger C. J. (2012). Relative detection efficiency of the world wide lightning location network. *Radio Science*, **47**(06), 1–9.
- Johnson G., Shalaev R., Hartnett R., Swaszek P. and Narins M. (2005). Can LORAN meet GPS backup requirements? *IEEE Aerospace and Electronic Systems Magazine*, **20**(2), 3–12.
- Johnson G., Wiggins M., Swaszek P. F., Hartshorn L. and Hartnett R. (2006). Possible optimizations for the us loran system. *Proceedings of IEEE/ION PLANS*, San Diego, 695–704.
- Klimov P. A., Kaznacheeva M. A., Khrenov B. A., Garipov G. K., Bogomolov V. V., Panasyuk M. I., Svertilov S. I. and Cremonini R. (2018). UV transient atmospheric events observed far from thunderstorms by the Vernov satellite. *IEEE Geoscience and Remote Sensing Letters*, **15**(8), 1139–1143.
- Lewin P. L., Tran T. N., Swaffield D. J. and Hallstrom J. K. (2008). Zero-phase filtering for lightning impulse evaluation: a K-factor Filter for the Revision of IEC60060-1 and -2. *IEEE Transactions on Power Delivery*, **23**(1), 3–12.
- Liu H., Qiu S. and Dong W. (2018). The three-dimensional locating of VHF broadband lightning interferometers. *Atmosphere (Basel)*, **9**(8), 1–14.
- Lo S. C., Peterson B. B. and Enge P. K. (2007). Loran data modulation: a primer. *IEEE AE Systems Magazine*, **22**(9), 31–51.
- Lojou J., Honma N., Cummins K. L., Said R. K. and Hembury N. (2011). Latest developments in global and total lightning detection. *2011 7th Asia-Pacific International Conference on Lightning*, Chengdu, China, 924–932.
- Morris P. B. and Casswell R. M. (1994). Evaluation of the 1993 Omega propagation correction model. In *Proceedings of 1994 IEEE Position, Location and Navigation Symposium - PLANS'94*, Las Vegas, NV, USA, 1994, 69–76.
- Narita T., Wanke E., Sato M., Sakanoi T., Kumada A., Kamogawa M., Hirohiko I., Harada S., Kameda T., Tsuchiya F. and Kaneko E. (2018). A study of lightning location system (Blitz) based on VLF sferics. *34th International Conference on Lightning Protection (ICLP)*, Rzeszow, Poland.
- Olsen D. L. (1991). Federal radionavigation policy and the land transportation user. *Vehicle Navigation and Information Systems Conference Troy, USA*, 627–634.
- Parmantier J. P., Issac F. and Gobin V. (2012). Indirect effects of lightning on aircraft and rotorcraft. *Journal of Aerospace Lab* (5), 1–27.
- Rakov V. A. and Uman A. (2007). *Lightning Physics and Effects*. Cambridge, England: Cambridge University Press.
- Rison W., Krehbiel P. L., Stock R. W., Edens H. E., Shao X., Thomas R. J., Stanley M. A. and Zhang Y. (2016). Observations of narrow bipolar events reveal how lightning is initiated in thunderstorms. *Nature communications*, **7**, 10721.
- Sakran F. C. and Swanson E. R. (1998). Omega: the end-what it was, what it did, what now? In *IEEE 1998 Position Location and Navigation Symposium*, Palm Springs, CA, USA, 85–92.
- Shao X. and Jacobson A. R. (2009). Model simulation of very low-frequency and low-frequency lightning signal propagation over intermediate ranges. in *IEEE Transactions on Electromagnetic Compatibility*, **51**(3), 519–525.
- Sonnadara U., Cooray V. and Fernando M. (2006). The lightning radiation field spectra of cloud flashes in the interval from 20 kHz to 20 MHz. *IEEE Transactions on Electromagnetic Compatibility*, **48**(1), 234–239.
- Sun Z., Qie X., Liu M., Cao D. and Wang D. (2013). Lightning VHF radiation location system based on short-baseline TDOA technique: validation in rocket-triggered lightning. *Atmospheric Research*, **129–130**, 58–66.
- Swanson E. R. (1983). Omega. *Proceedings of the IEEE*, **71**(10), 1140–1155.
- Warren R. S., Morris P. B., Gupta R. R. and Desrochers G. R. (1992). Omega system performance assessment. In *IEEE PLANS 92 Position Location and Navigation Symposium Record*, Monterey, CA, USA, 88–95.
- Wenzel R. J. (1989). Omega: system status update-1988. *Aerospace and Electronic Systems Magazine IEEE*, **4**(7), 24–33.
- Yuan J., Yan W., Li S. and Hua Y. (2020). Demodulation method for Loran-C at low SNR based on envelope correlation-phase detection. *Sensors*, **20**, 4535.